

Photoabsorption and photoemission of Cu near the 3*p* threshold

L. C. Davis and L. A. Feldkamp

Engineering and Research Staff, Ford Motor Company, Dearborn, Michigan 48121

(Received 22 June 1981)

The photoabsorption and photoemission of Cu in the region of the 3*p* threshold have been calculated. The resonance in the Cu⁺ 3*d*⁸4*s*² emission due to super-Coster-Kronig decay is found to occur primarily in the ¹G multiplet (62%) with lesser amounts in ³F and ¹D (29% and 8%). We find a comparatively large nonresonant emission due to inelastic scattering into 3*d*⁹4*p* final states which occurs at approximately the same binding energy as 3*d*⁸4*s*²³F. Shake-up processes, in particular those leading to 3*d*⁹5*s*, are shown to be important. It is concluded that interference in the 3*p*→*nd*, *εd* channel leads to the dip in absorption found above the 3*p*→4*s* peaks.

I. INTRODUCTION

Considerable attention has been given to the 3*p*→3*d* excitation in the transition metals.¹⁻⁵ The peaks in absorption are asymmetric and broad due to Fano resonances,⁶ which exist because excited states of configuration 3*p*⁵3*d*^{*n*+1}4*s*² decay via super-Coster-Kronig (sCK) transitions⁷ to final states 3*p*⁶3*d*^{*n*-1}4*s*²*εl* (autoionization). These final states can also be excited directly from the ground state, 3*p*⁶3*d*^{*n*}4*s*², causing interference. Both the large width and the prominent asymmetry are due to the strength of the sCK matrix elements.

In Cu, the 3*d* subshell is full and the absorption is due to the weaker 3*p*→4*s* transitions. The excited states, which are 3*p*⁵3*d*¹⁰4*s*², can decay via sCK transitions to 3*p*⁶3*d*⁹4*s*²*εl*, giving appreciable width. However, the direct excitation of the Cu⁺ 3*d*⁸4*s*² final states is weak because it is a two-electron transition. Consequently, we expect negligible interference from this source. As we shall show, the Auger decay to 3*p*⁶3*d*⁹4*s**εl* is weak enough that only a small amount of interference occurs, even though the direct excitation of these states is the dominant photoionization process. Hence we expect a symmetric line shape.

The absorption data of Bruhn, Sonntag, and Wolff⁵ (shown in Fig. 1), on the other hand, appear to show a dip above the 3*p*→4*s* peaks. This could be due to a negative Fano *q* parameter (line profile index), or possibly a positive *q* associated with higher energy transitions, such as 3*p*→5*s*, 3*p*→4*d*, 3*p*→*εl*, etc. Yafet⁸ has discussed the effects of shake-up transitions, which might cause interference. These and other processes will be considered.

Recently, Chandesris and co-workers⁹ measured the Cu photoemission in this range of photon energy. At a given *hν*, the photoemission intensity integrated over kinetic energy and solid angle (of the escaping electron) equals the absorption, since radiative decay and inelastic collisions with other atoms can be neglected. Photoemission spectra

contain detailed information about the excitation of individual final states which is not evident in absorption. Cu is a good example to consider, since its electronic structure is simple (in the present context) and the analysis of its spectra should be straightforward, providing a test of currently accepted ideas.

In this paper, we calculate the photoabsorption and photoemission of Cu and compare to experiment. We use the Fano formalism to treat the resonance and autoionization aspects of the problem. The majority of the computations are based upon multiplet theory using radial orbitals (bound and continuum) determined from the Herman-Skillman (HS) (Ref. 10) potential for the ground state of Cu. We also examine the effects of configuration interaction (CI), inelastic scattering in the final states, and shake-up.

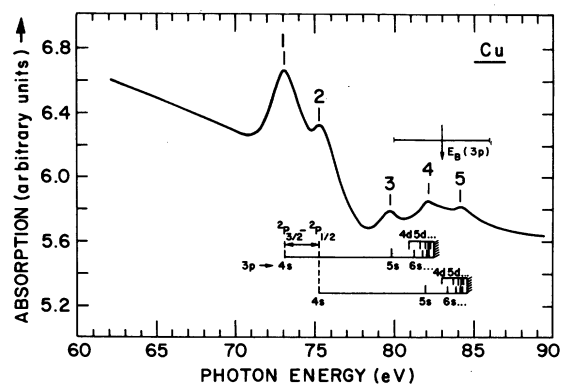


FIG. 1. Absorption spectrum of Cu vapor measured by Bruhn, Sonntag, and Wolff (Ref. 5). Peaks 1 and 2 correspond to the excitation of 3*p*⁵3*d*¹⁰4*s*²2*P*_{3/2,1/2}. The tentative assignment of higher energy peaks (after Ref. 5) is in analogy to Zn 3*d*¹⁰4*snl* excited states, e.g., peak 3 corresponds to 3*p*⁵3*d*¹⁰4*s*5*s*²2*P*_{3/2}. The binding energy of a 3*p* hole is estimated to be 83±3 eV (Ref. 18).

II. FROZEN-ORBITAL MULTIPLET THEORY

In this section we calculate photoabsorption and photoemission of Cu in the region of the $3p$ threshold ($\sim 70-80$ eV). The formal theory is based upon our extension^{11,12} of Fano's formalism⁶ for the interaction of discrete and continuum states. To describe the wave functions, we use single configuration multiplet theory, retaining the same basis set for the ground state, discrete excited states, and continuum final states. In numerical calculations, we employ HS orbitals obtained from the ground-state potential (with the Latter tail¹⁰). Improvements are discussed in Sec. III.

A. Theory ($3p \rightarrow 4s$)

The ground state Φ_g has configuration $3p^6 3d^{10} 4s^2 ({}^2S_{1/2})$. We take the $4s$ electron to be spin \uparrow

$$\Phi_g = |3p^6 3d^{10} 4s \uparrow\rangle. \quad (1)$$

In the notation of Refs. 11 and 12, the discrete states are denoted by ϕ_n and correspond to $3p^5 3d^{10} 4s^2 P_{1/2,3/2}$. Let $j(m_j)$ be the total angular momentum (z component) of the $3p$ core hole, so that n stands for jm_j ,

$$\phi_n = |3p^5(jm_j) 3d^{10} 4s^2\rangle. \quad (2)$$

There are two types of continuum states. The first has configuration $3p^6 3d^8 4s^2 \epsilon l$. The $3d^8$ part is treated in LS coupling and has quantum numbers $LSM_L M_S$. The continuum orbital is ϵl where $l=1, 3$, or 5 . The z components of its orbital angular momentum and spin are m_l and m_s . Letting k stand for $LSM_L M_S l m_l m_s$, we have

$$\psi_{kE} = |3p^6 3d^8(LSM_L M_S) 4s^2 \epsilon l m_l m_s\rangle. \quad (3)$$

Here $E = \epsilon + E_{LS}$, where E_{LS} is the energy of the $\text{Cu}^+ 3d^8 4s^2 2S+1L$ ion. These states are the principal final states resulting from the sCK decay of the discrete excited states.

The second type of continuum state is $3p^6 3d^9 4s^{1,3} D \epsilon l$ where $l=1$ or 3 . These states give most of the $3d$ photoionization. We treat the $3d^9 4s$ part in LS coupling (quantum numbers $L=2, SM_L M_S$). Letting k here stand for $SM_L M_S l m_l m_s$, we denote these states as

$$\psi'_{kE} = |3p^6 3d^9 4s(SM_L M_S) \epsilon' l m_l m_s\rangle. \quad (4)$$

$E = \epsilon' + E_S$, where E_S is the energy of $\text{Cu}^+ 3d^9 4s^{2S+1} D$. The weak photoemission and Auger decay associated with $\text{Cu}^+ 3d^{10}$ is neglected.

Since the dipole matrix element between Φ_g and ψ_{kE} [Eq. (3)] vanishes, only ψ'_{kE} enters the computation of the q parameter. For $3p-4s$, the decay matrix Γ is diagonal in jm_j , so that the analysis reduces to that of Fano's case for one discrete state interacting with several continua.⁶ Further-

more, q is independent of j and m_j

$$\frac{1}{q} = -2\pi \sum_{i=1,3} \langle l100 | 20 \rangle^2 (\epsilon' l | r | 3d) [R_i(3p, \epsilon' l; 3d, 4s) - \frac{2}{3} (2l+1) R_1(3p, \epsilon' l; 4s, 3d)] / (4s | r | 3p), \quad (5)$$

where the radial integrals are

$$(a | r | b) = \int_0^\infty r^3 dr R_a(r) R_b(r) \quad (6)$$

and

$$R_K(a, b; c, d) = \int_0^\infty r_1^2 dr_1 \int_0^\infty r_2^2 dr_2 R_a(r_1) R_b(r_2) \times \frac{r_{<}^K}{r_{>}^{K+1}} R_c(r_1) R_d(r_2). \quad (7)$$

Throughout, we shall use atomic units unless specified otherwise. [In deriving (5) we have neglected the difference between ϕ_n and $\bar{\phi}_n$ of Ref. 11.] $\langle j_1 j_2 m_1 m_2 | JM \rangle$ is a Clebsch-Gordan coefficient.

The width Γ (FWHM = 2Γ) is the sum of the sCK decay into ψ_{kE} [Eq. (3)] and the Auger decay into ψ'_{kE} [Eq. (4)]

$$\Gamma = \sum_{iLS} \Gamma_{iLS} + \sum_{iS} \Gamma_{iS}. \quad (8)$$

Γ is also independent of j and m_j . Γ_{iLS} in (8) represents the decay into the LS multiplet of $\text{Cu}^+ 3d^8 4s^2$ with an ϵl photoelectron and is given by

$$\Gamma_{iLS} = 50\pi(2l+1)(2L+1)(2S+1) \times \left(\sum_{K=1,3} \frac{1}{2K+1} R_K(3p, \epsilon l; 3d, 3d) \times \langle 1200 | K0 \rangle \langle 1200 | K0 \rangle \begin{Bmatrix} l & 1 & L \\ 2 & 2 & K \end{Bmatrix} \right)^2, \quad (9)$$

where $\begin{Bmatrix} j_1 & j_2 & j_3 \\ j_1 & j_2 & j_3 \end{Bmatrix}$ is a $6j$ symbol. Γ_{iS} is the decay into $3d^9 4s^{2S+1} D$ and is given by

$$\Gamma_{iS} = \pi \frac{2S+1}{2l+1} \langle l100 | 20 \rangle^2 [R_i(3p, \epsilon' l; 3d, 4s) + (-1)^S \frac{2l+1}{3} \times R_1(3p, \epsilon' l; 4s, 3d)]^2. \quad (10)$$

Typically, the Γ_{iLS} are much larger than the Γ_{iS} .

We next find the photoemission intensity integrated over solid angle for various final states. It is convenient to use units of $2\pi |\bar{\mathbf{E}}_0|^2$, where $\bar{\mathbf{E}}_0$ is the complex electric field amplitude. Letting the ground-state energy be zero, we have $E = h\nu$. We average over polarization of the photon. For $3d^9 4s^{2S+1} D$ final states, we find (summing over M_L, M_S, l, m_l , and m_s)

$$\begin{aligned}
N_S(E) = & \frac{2S+1}{6} \left[\sum_{l=1,3} (2l+1) \langle l100 | 20 \rangle^2 (\epsilon'l | r | 3d)^2 \right. \\
& + 4 \sum_{l=1,3} \langle l100 | 20 \rangle^2 (\epsilon'l | r | 3d) (4s | r | 3p) \left((-1)^S R_l(3p, \epsilon'l; 3d, 4s) \right. \\
& \left. \left. + \frac{2l+1}{3} R_l(3p, \epsilon'l; 4s, 3d) \right) \sum_{j=\frac{1}{2}, \frac{3}{2}} \left(\frac{2j+1}{6} \right) \frac{E-E_j-\Gamma/q}{(E-E_j)^2 + \Gamma^2} \right] \\
& + \left(\sum_{l=1,3} \Gamma_{ls} \right) \frac{(4s | r | 3p)^2}{3\pi\Gamma^2} \left(1 + \frac{1}{q^2} \right) \sum_{j=\frac{1}{2}, \frac{3}{2}} \left(\frac{2j+1}{6} \right) \frac{\Gamma^2}{(E-E_j)^2 + \Gamma^2}. \quad (11)
\end{aligned}$$

In (11) and subsequent equations, E_j refers to the energy of $3p^5 3d^{10} 4s^2 2^2 P_j$. Likewise for $3d^8 4s^2 2^2 S^+ L$, we have

$$N_{LS}(E) = \left(\sum_l \Gamma_{lLS} \right) \frac{(4s | r | 3p)^2}{3\pi\Gamma^2} \left(1 + \frac{1}{q^2} \right) \sum_{j=\frac{1}{2}, \frac{3}{2}} \left(\frac{2j+1}{6} \right) \frac{\Gamma^2}{(E-E_j)^2 + \Gamma^2}. \quad (12)$$

The absorption is simply the total emission¹³

$$W(E) = \sum_{LS} N_{LS}(E) + \sum_S N_S(E) \quad (13)$$

$$= \sum_{l=1,3} \frac{2}{3} (2l+1) \langle l100 | 20 \rangle^2 (\epsilon'l | r | 3d)^2 + \frac{(4s | r | 3p)^2}{3\pi\Gamma} \frac{1}{q^2} \left(\sum_j \frac{2j+1}{6} \frac{[q + (E-E_j)/\Gamma]^2}{1 + (E-E_j)^2/\Gamma^2} - 1 \right). \quad (14)$$

For comparison to other calculations, we note that the photoabsorption cross section in Mb can be written as (E in Ry)

$$\sigma = 0.856(3\pi E)W(E) \quad (15)$$

and the spectral density of oscillator strength (in eV^{-1} with E in Ry) as

$$\frac{df}{dE} = \frac{EW(E)}{13.606}. \quad (16)$$

B. Numerical results ($3p \rightarrow 4s$)

To calculate the absorption and photoemission, we have evaluated the parameters such as $\langle \epsilon'l | r | 3d \rangle$, $R_K(3p, \epsilon'l; 3d, 3d)$, etc., using radial wave functions obtained from the HS potential for the ground state of the Cu atom. Our values,¹⁴ listed in Table I, compare reasonably well with

TABLE I. Parameters in atomic units using Herman-Skillman wave functions for neutral Cu ($\epsilon' = 4.65$ Ry and $\epsilon = 4.12$ Ry).

$\langle 4s r 3p \rangle = 0.1847$
$\langle \epsilon'p r 3d \rangle = 0.0625$
$\langle \epsilon'f r 3d \rangle = 0.3193$
$R_1(3p, \epsilon'p; 3d, 4s) = 0.0338$
$R_3(3p, \epsilon'f; 3d, 4s) = 0.0178$
$R_1(3p, \epsilon'p; 4s, 3d) = 0.0126$
$R_1(3p, \epsilon'f; 4s, 3d) = 0.0612$
$R_1(3p, \epsilon p; 3d, 3d) = 0.0139$
$R_3(3p, \epsilon p; 3d, 3d) = 0.0150$
$R_1(3p, \epsilon f; 3d, 3d) = -0.1053$
$R_3(3p, \epsilon f; 3d, 3d) = -0.0522$

those given by McGuire.^{7,15} (We neglect ϵh orbitals since their contribution is small.)

As a preliminary, we have listed in Tables II and III oscillator strengths and photoabsorption cross sections calculated from strictly one-electron theory. No interference or decay has been included. Experimental transition energies have been used. The predominant photoabsorption (photoionization) is $3d \rightarrow \epsilon f$.

When we include the effects discussed in Sec. II A, we find the results displayed in Table IV and in Figs. 2 and 3. The calculated line width is 3.42 eV (FWHM) which is about twice the experimental value. McGuire¹⁵ has suggested that this discrepancy results from the use of the HS potential for the ϵl continuum orbitals instead of the more correct Hartree-Fock (HF) potential. The calculated value of q is 26.6 (as given in Table V), which demonstrates that the Auger decay to $3d^9 4s$ final states does not give much interference. Consequently, the apparent dip in the absorption above the $3p \rightarrow 4s$ peaks is not due to this process. Most of the width comes from sCK transitions to $3d^9 4s^2$.

In Fig. 2, we show the photoemission intensity for various final states as a function of photon energy. Since our calculated Γ is too large, the spin-orbit splitting is not as well resolved in the calculations as in the experiment. The curve marked "Total" corresponds to the absorption $W(E)$. The variation of the dipole and Coulomb matrix elements as a function of ϵ ($= h\nu - \text{const}$) is small over the range shown and has been neglected. Transitions to higher-lying states are considered in Sec. II C. The value of $W(E)$ in the absence

TABLE II. Oscillator strengths.

$3p \rightarrow 4s$	5s	6s	ϵs ($\epsilon = 0.1$ Ry)
$f = 0.0618$	0.0186	6.36×10^{-3}	$df/dE = 8.56 \times 10^{-3} \text{ eV}^{-1}$
$3p \rightarrow 4d$			ϵd ($\epsilon = 0.1$ Ry)
$f = 0.00325$			$df/dE = 4.02 \times 10^{-3} \text{ eV}^{-1}$
$3d \rightarrow \epsilon p$		ϵf	total ($\epsilon = 4.65$ Ry)
$df/dE = 2.08 \times 10^{-3} \text{ eV}^{-1}$		$8.15 \times 10^{-2} \text{ eV}^{-1}$	$8.36 \times 10^{-2} \text{ eV}^{-1}$

of the $3p \rightarrow 4s$ transitions is 0.2091. The peak value at resonance is 0.2314, an increase of 11% which is comparable to, but larger than, the corresponding experimental value. Since our width Γ is too large, the calculated oscillator strength for $3p \rightarrow 4s$ relative to the background ($3d \rightarrow \epsilon l$) is more than a factor of 2 too large. Such discrepancies in cross sections calculated with the HS potential are not uncommon.¹⁶ Also, it is not clear that the normalization procedures employed in Ref. 5 necessarily preserve the zero of intensity (i.e., obtain a correct representation of the background).

The intensity of the $3d^8 4s^2$ final states is shown in more detail in Fig. 3. The percentage of the $3d^8 4s^2$ emission in 1G is 62%, in 3F 29%, and in 1D 8%. The 3P and 1S intensities are negligible.

According to the Moore's tables,¹⁷ the $\text{Cu}^+ 3d^9 4s$ 3D final states have binding energies 10.4, 10.6, and 10.7 eV for the $J=3, 2,$ and 1 components, respectively. The 1D state is at 11.0 eV. No other levels are close in binding energy. However, the $3d^8 4s^2$ multiplets ($^3F=16.5$ eV, $^1D=18.3$ eV, and $^1G=19.6$ eV) are close to other states (e.g., $3d^9 4p$) which have some intensity and may make interpretation of photoemission experiments difficult (see Sec. III).

TABLE III. Photoabsorption cross sections (Mb). $\sigma_0(E) = 0.856(3\pi E)$ with $E = h\nu$ in Ry.

$\sigma_{3d \rightarrow 4s} = \sigma_0(E) \frac{4}{3} (\epsilon p r 3d)^2 = 0.229$	
$\sigma_{3d \rightarrow \epsilon f} = \sigma_0(E) 2(\epsilon f r 3d)^2 = 8.947$	($\epsilon = 4.65$ Ry, $h\nu = 74$ eV)
$\sigma_{3d} = 9.18$	
$\sigma_{3p \rightarrow \epsilon s} = \sigma_0(E) \frac{2}{3} (\epsilon s r 3p)^2 = 0.940$	($\epsilon = 0.1$ Ry, $h\nu = 83$ eV)
$\sigma_{3p \rightarrow \epsilon d} = \sigma_0(E) \frac{4}{3} (\epsilon d r 3p)^2 = 0.441$	
$\sigma_{3p} = 1.38$	

C. $3p \rightarrow 5s, 4d, \dots, \epsilon l$

Above the principal resonances in absorption (peaks at 73 and 75 eV) is structure attributed⁵ to $3p \rightarrow 5s, 4d, 6s, \dots$ based upon a comparison to the $\text{Zn } 3d^{10} 4s n l$ energy levels. In this region of energy, the $3p \rightarrow \epsilon s, d$ thresholds also occur (estimated¹⁸ to be ~ 83 eV). We calculate the contribution of these transitions to the absorption in this section.

For $3p \rightarrow ns$, $n=5, 6, \dots$ we find in analogy to (14)

$$W_{ns}(E) = \frac{2(ns|r|3p)^2}{3\pi\Gamma} \frac{1}{q_{ns}^2} \times \left[\sum_{j=\frac{1}{2}, \frac{3}{2}} \left(\frac{2j+1}{6} \right) \frac{[q_{ns} + (E - E_j^{ns})/\Gamma]^2}{1 + (E - E_j^{ns})^2/\Gamma^2} - 1 \right], \quad (17)$$

where q_{ns} is given by (5) with $4s$ replaced by ns . E_j^{ns} is the energy of the $3p^5 3d^{10} 4s n l$ excited state

TABLE IV. Calculated widths for $3p^5 3d^{10} 4s^2$ (in atomic units unless noted otherwise).

S	Γ_{ps}	Γ_{fs}	$\sum \Gamma_{is}$
0	0.2995×10^{-2}	0.3966×10^{-3}	0.3392×10^{-2}
1	0.1882×10^{-2}	0.1471×10^{-4}	0.1897×10^{-2}
			Total = 0.5288×10^{-2}
$2s^4 L$	Γ_{pLS}	Γ_{fLS}	$\sum \Gamma_{iLS}$
1S	0.618×10^{-3}	0	0.618×10^{-3}
3P	0.425×10^{-3}	0	0.425×10^{-3}
1D	0.543×10^{-3}	0.9082×10^{-2}	0.9624×10^{-2}
3F	0	0.3457×10^{-1}	0.3457×10^{-1}
1G	0	0.7508×10^{-1}	0.7508×10^{-1}
			Total = 0.1203
$\Gamma = 0.1256$ a.u.		$2\Gamma(\text{FWHM}) = 3.42$ eV	

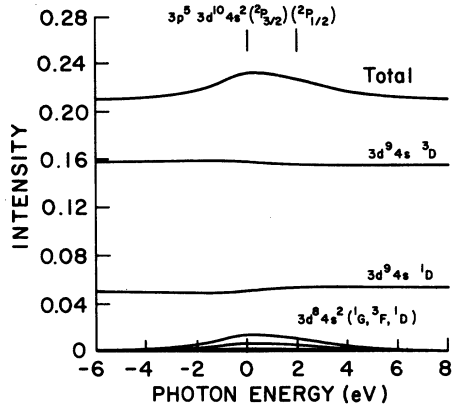


FIG. 2. Calculated photoemission intensity vs photon energy relative to $3p^5 3d^{10} 4s^2 2P_{3/2}$ threshold (73.15 eV) for various Cu^+ final states. To obtain intensity in atomic units, multiply by $2\pi |\vec{E}_0|^2$. The curve marked "Total" equals absorption with a cross section σ of 9.7 Mb at the peak. The parameters are evaluated at $h\nu = 74$ eV using Herman-Skillman radial wave functions. The spin orbit splitting is taken to be 2 eV.

with a $3p_j$ hole (including resonance shift). Γ is taken to be the same as for $3p \rightarrow 4s$, since both are dominated by the identical sCK transitions.

The pertinent parameters for the evaluation of (17) are given in Table VI and previous tables. The value of q for $5s$ (Table V) is large (34.1), indicating little interference. The oscillator strength (Table II) $f_{3p \rightarrow 5s}$ is 30% of $f_{3p \rightarrow 4s}$, which is consistent with identifying the peak at 80 eV

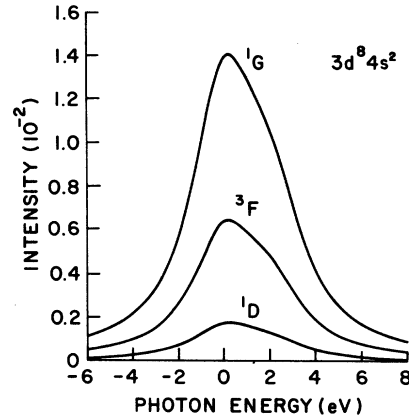


FIG. 3. Calculated photoemission intensity for $\text{Cu}^+ 3d^8 4s^2$ final states on expanded scale. 3P and 1S are negligible.

(number 3) in the experimental spectrum with $3p_{3/2} \rightarrow 5s$. The oscillator strength $f_{3p \rightarrow 6s}$ is 10% of $f_{3p \rightarrow 4s}$, an observable amount which could well be part of the peaks at 82 and 84 eV (numbers 4 and 5).

For $3p \rightarrow nd, n=4, 5, \dots$ we find

$$W_{nd} = \frac{4(nd|r|3p)^2}{3\pi\Gamma} \frac{1}{q_{nd}^2} \times \left[\sum_{j=\frac{1}{2}, \frac{3}{2}} \left(\frac{2j+1}{6} \right) \frac{[q_{nd} + (E - E_j^{nd})/\Gamma]^2}{1 + (E - E_j^{nd})^2/\Gamma^2} - 1 \right], \quad (18)$$

where

$$\frac{1}{q_{nd}} = -\frac{6\pi}{(nd|r|3p)} \left\{ (\epsilon p |r| 3d) \left[\frac{1}{45} R_1(3p, \epsilon p; 3d, nd) + \frac{3}{35} R_3(3p, \epsilon p; 3d, nd) - \frac{4}{9} R_1(3p, \epsilon p; nd, 3d) \right] \right. \\ \left. + (\epsilon f |r| 3d) \left[\frac{1}{5} R_1(3p, \epsilon f; 3d, nd) + \frac{2}{35} R_3(3p, \epsilon f; 3d, nd) - \frac{2}{9} R_1(3p, \epsilon f; nd, 3d) \right] \right\}. \quad (19)$$

From Table II, we see that the oscillator strength $f_{3p \rightarrow 4d}$ (in the absence of interference) is 5% of $f_{3p \rightarrow 4s}$. The q value is 1.64, which represents appreciable interference. The dip-to-peak

TABLE V. Fano asymmetry parameters.

Discrete state (2P_j)	q
$3p^5 3d^{10} 4s^2$	26.6
$3p^5 3d^{10} 4s 5s$	34.1
$3p^5 3d^{10} 4s 4d$	1.64
$3p^5 3d^{10} 4s \epsilon d$ ($\epsilon = 0.1$ Ry)	0.69

distance in $W(E)$ is $1 + 1/q^2 = 1.4$ times the peak height when $q \rightarrow \infty$. This is about 7% of the $3p \rightarrow 4s$ peak height (above background) and is comparable to the $3p \rightarrow 6s$ peak height. Although $3p \rightarrow 4d$ transitions contribute to the 82 and 84 eV peaks, the oscillator strength is not large enough for this interference by itself to cause an appreciable dip on the high-energy side of the $3p \rightarrow 4s$ peaks.

The cross section σ_{3p} for $3p \rightarrow \epsilon l$ absorption near threshold is approximately 15% of the background σ_{3d} (Table III), in the absence of interference and decay. It is comparable to the increase in absorption at the $3p \rightarrow 4s$ resonance. (Our results for

TABLE VI. Parameters in atomic units.

$(5s r 3p)=0.0684$
$\epsilon' = 5.14$
$(\epsilon'p r 3d)=0.0605$
$(\epsilon'f r 3d)=0.2948$
$R_1(3p, \epsilon'p; 3d, 5s)=0.0127$
$R_3(3p, \epsilon'f; 3d, 5s)=6.87 \times 10^{-3}$
$R_1(3p, \epsilon'p; 5s, 3d)=4.86 \times 10^{-3}$
$R_1(3p, \epsilon'f; 5s, 3d)=2.22 \times 10^{-3}$
$(4d r 3p)=-0.0200$
$\epsilon = 4.65$
$(\epsilon p r 3d)=0.0618$
$(\epsilon f r 3d)=0.3198$
$R_1(3p, \epsilon p; 3d, 4d)=9.71 \times 10^{-4}$
$R_3(3p, \epsilon p; 3d, 4d)=9.93 \times 10^{-4}$
$R_1(3p, \epsilon p; 4d, 3d)=9.17 \times 10^{-4}$
$R_1(3p, \epsilon f; 3d, 4d)=-3.41 \times 10^{-3}$
$R_3(3p, \epsilon f; 3d, 4d)=-1.76 \times 10^{-3}$
$R_1(3p, \epsilon f; 4d, 3d)=-4.29 \times 10^{-3}$
$(6s r 3p)=0.0393$

$\sigma_{3p \rightarrow \epsilon l}$ are in good agreement with those of Manson and Cooper.¹⁹ Hence, we conclude that much of the increase of the absorption in the range 77–85 eV is due to the onset of continuum transitions. Furthermore, if we calculate an asymmetry parameter q using (19) with nd replaced by ϵd , we find near threshold that $q=0.69$. This represents a sizeable interference in a relatively large term. We conclude, therefore, that most of the dip in the absorption results from interference in the $3p \rightarrow \epsilon d$ channel.

To calculate the $3p \rightarrow \epsilon d$ absorption including interference and decay,²⁰ we replace nd by ϵd in (18) and integrate over ϵ . E_j^{nd} becomes $E_{Bj} + \epsilon$, where E_{Bj} is the binding energy of the $3p$, hole including resonance shift and q is, in principle, a function of ϵ . To determine the form near threshold, we use the approximate procedure of setting $(\epsilon d|r|3p)$ and q equal to their values at $\epsilon=0$. It is necessary to introduce a cutoff in the integration over ϵ since the integrand goes as $1/\epsilon$ for $\epsilon \rightarrow \infty$. The result is

$$W_d(E) \approx \frac{4}{3} (\epsilon=0d|r|3p)^2 \sum_{j=\frac{1}{2}, \frac{3}{2}} \left(\frac{2j+1}{6} \right) \left\{ \left(1 - \frac{1}{q^2} \right) \left[1/2 + \frac{1}{\pi} \tan^{-1} \left(\frac{E - E_{Bj}}{\Gamma} \right) \right] + \frac{1}{\pi q} \ln \left[1 + \left(\frac{E - E_{Bj}}{\Gamma} \right)^2 \right] \right\} + \text{const.} \quad (20)$$

The width Γ could be different (probably larger¹⁵ than the width for $3p \rightarrow 4s$ because the final states are now Cu^{2*}). Only the constant term in (20) depends upon the cutoff.

The $3p \rightarrow \epsilon s$ absorption is given by a similar expression with $\frac{2}{3} (\epsilon s|r|3p)^2$ replacing $\frac{4}{3} (\epsilon d|r|3p)^2$ in (20). Since the interference in this channel is small, one can take the $q \rightarrow \infty$ limit to obtain for E near $E_B(3p)$

$$W_s(E) \approx \frac{2}{3} (\epsilon=0s|r|3p)^2 \times \sum_{j=\frac{1}{2}, \frac{3}{2}} \left(\frac{2j+1}{6} \right) \left[1/2 + \frac{1}{\pi} \tan^{-1} \left(\frac{E - E_{Bj}}{\Gamma} \right) \right]. \quad (21)$$

In Fig. 4, we show the absorption (apart from the background) obtained by combining the contributions for $4s$, $5s$, $6s$, ϵs , $4d$, and ϵd . We have scaled Γ by 2 to agree with experiment and have chosen the E_j^{nd} energies to reproduce the measured spectrum. We have used our calculated oscillator strengths and q values. The most critical choice is E_{Bj} , the $3p$ threshold including resonance shift. For the figure we have taken $E_{B3/2} = 80$ eV (i.e., 7 eV above the $4s$ peak $E_{3/2} = 73$ eV), which is below $E_{3/2}^{4d}$ and $E_{3/2}^{6s}$. For this choice to be sensible, a larger resonance shift is required for states $3p^5 3d^{10} 4s \epsilon l$ than for $3p^5 3d^{10} 4s n l$, which seems unlikely. This may indicate that the correct expression for the threshold absorption dif-

fers in detail from the form used here, or perhaps that the distribution of oscillator strength among bound and continuum orbitals is not given accurately by the HS wave functions. Conceivably, the discrete structure is due to some other type of transition. In any event, Fig. 4 agrees reason-

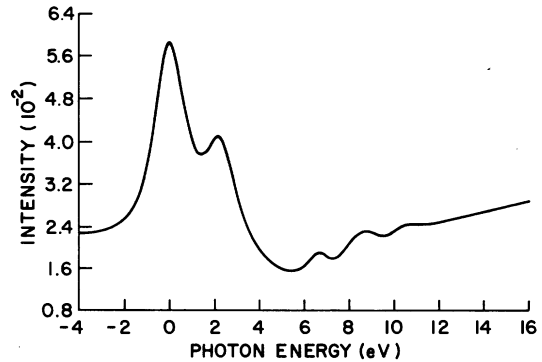


FIG. 4. Calculated absorption (suppressed zero) including $3p \rightarrow 4s$, $5s$, $6s$, ϵs , $4d$, and ϵd transitions. Oscillator strengths and q values are calculated from HS ground-state potential. The $\text{FWHM} = 2\Gamma = 1.71$ eV is $\frac{1}{2}$ of the calculated value (used in Figs. 1 and 2). The spin-orbit splitting has been taken to be 2.25 eV. Energy levels including resonance shift relative to $4s$ for each j : $5s = 6.65$ eV; $4d = 7.8$ eV; $6s = 8.2$ eV; ϵs and ϵd threshold = 7.0 eV. Strong interference in $3p \rightarrow \epsilon d$ channel causes the dip in absorption above $4s$ peaks.

ably well with the data of Bruhn *et al.* (Fig. 1), especially if we add an energy-dependent background.

The intensity of the $\text{Cu}^+ 3d^9 4s 1^3D$ photoemission, $N_s(E)$, should show a dip below $E_B(3p)$ due to the interference from the $3p \rightarrow \epsilon d$ channel. Following Yafet,¹³ we expect the effective asymmetry parameter \bar{q} to be small ($\bar{q} < q$), since $N_s(E)$ plus the Auger emission (final states $\text{Cu}^{2+} 3d^8 4s$), which is Lorentzian, must give an absorption characterized by $q = 0.69$. To test experimentally for interference in the $3p \rightarrow \epsilon d$ channel, it would be interesting to measure the photoemission into ϵd near $\epsilon = 0$ and $E \sim E_B(3p)$. The emission should have a Fano form. It can be shown that (for each j)

$$N_s(E) \approx \frac{4}{3} (\epsilon = 0d | r | 3p)^2 \left(\frac{2j+1}{6} \right) \frac{\Theta(\epsilon) (q + \delta)^2}{\pi q^2 \Gamma (1 + \delta^2)}, \quad (22)$$

where $\delta = (E - E_{Bj} - \epsilon)/\Gamma$ and $\Theta(\epsilon)$ is the unit step function. Hence, a minimum occurs at $\delta = -q$ or $\epsilon = E - E_{Bj} + q\Gamma$. The discrete states do not contribute to the current at $\epsilon \approx 0$ unless there is an additional decay $3p^5 3d^{10} 4s nd - 3p^5 3d^{10} 4s \epsilon d$.

III. IMPROVEMENTS AND EXTENSIONS

In this section we describe improvements in the theory and calculations given in Sec. II. Rough estimates of the magnitudes of the effects of configuration interaction (CI), multielectron transitions, shake-up processes, and inelastic scattering are given.

From a computational point of view, the most serious error is probably the use of HS orbitals, particularly for continuum wave functions. Kennedy and Manson²¹ have compared photoabsorption cross sections calculated using HS and Hartree-Fock (HF) orbitals. In some instances, considerable differences were found. The formalism presented in Sec. II A would, of course, still hold if HF orbitals were used.

Starace¹⁶ has reviewed various techniques which go beyond HF theory. Calculations of this nature are beyond the scope of the present work. However, we attempt to isolate some of the important effects using perturbation theory and simple considerations. Systematic treatment of such problems and an alternative formalism has been given by Wendin and co-workers.²²

Let us begin with some general considerations

$$\sum_k |\psi_{kE}\rangle \langle \psi_{kE}| = \sum_k |\psi_{kE}^{(0)}\rangle \langle \psi_{kE}^{(0)}| + \sum_{k,k'} P \int \frac{dE'}{E - E'} [U_{k'k}(E', E) |\psi_{k'E'}^{(0)}\rangle \langle \psi_{kE}^{(0)}| + U_{kk'}(E, E') |\psi_{kE}^{(0)}\rangle \langle \psi_{k'E'}^{(0)}|] + \dots \quad (28)$$

The real inelastic scattering represented by the imaginary part of $1/(E - E' - i\delta)$ in (27) (i.e., $i\pi\delta(E - E')$) does not contribute to (27) as noted above and, consequently, has no effect on $W(E)$.

concerning improvements on the continuum states ψ_{kE} due to shake-up, CI, and inelastic scattering. To obtain the correct photoemission for each final state [e.g., $N_{LS}(E)$ for $3d^8 4s^{2s+1}L$], it is obviously essential to have the correct ψ_{kE} . However, for the absorption less stringent requirements exist because the absorption is the total photoemission from all final states and is not sensitive to the distribution among outgoing channels. Formally, this follows from the fact that the continua always enter the absorption in the form $\sum_k |\psi_{kE}\rangle \langle \psi_{kE}|$ [see Eqs. (53) and (54) of Ref. 11].

For example, suppose that the zero-order approximation is of the form (as in Sec. II.)

$$\psi_{kE}^{(0)} = |\epsilon, \Phi_k^{(0)}\rangle, \quad \epsilon = E - E_k^{(0)}, \quad (23)$$

where $E_k^{(0)}$ is the energy of the ion in state $\Phi_k^{(0)}$ and ϵ represents the photoelectron. Let the final-state interaction (shake-up, real inelastic scattering, etc.) mix the zero-order continua according to

$$\psi_{kE} = \sum_{k'} C_{kk'}(E) \psi_{k'E}^{(0)} \quad (24a)$$

$$= \sum_{k'} C_{kk'}(E) |\epsilon = E - E_{k'}^{(0)}, \Phi_{k'}^{(0)}\rangle, \quad (24b)$$

where $C_{kk'}(E)$ is unitary. Under these conditions

$$\sum_k |\psi_{kE}\rangle \langle \psi_{kE}| = \sum_k |\psi_{kE}^{(0)}\rangle \langle \psi_{kE}^{(0)}| \quad (25)$$

and the absorption is unaffected. If instead of (24), we have CI in the ion states so that the new $\Phi_k = \sum_{k'} C_{kk'} \Phi_{k'}^{(0)}$ and $\psi_{kE} = |\epsilon, \Phi_k\rangle$, (25) no longer holds rigorously but is still approximately true if the relevant matrix elements (e.g., $\sum_k \langle \phi_n | \hat{H} | \psi_{kE}\rangle \langle \psi_{kE} | T | \Phi_k \rangle$) do not depend strongly on ϵ .

An important type of final-state interaction is inelastic scattering of the outgoing photoelectron (e.g., $3d^9 4s \epsilon f - 3d^9 4p \epsilon' d$). It can be treated by adding a term to the Hamiltonian matrix for the continuum states¹¹

$$\langle \psi_{kE}^{(0)} | \hat{H} | \psi_{k'E'}^{(0)} \rangle = E \delta_{kk'} \delta(E - E') + U_{kk'}(E, E'). \quad (26)$$

The new continuum states are (treating U as a perturbation)

$$\psi_{kE} = \psi_{kE}^{(0)} + \int \frac{dE'}{E - E' - i\delta} \sum_{k'} U_{k'k}(E', E) \psi_{k'E'}^{(0)} + \dots \quad (27)$$

It is straightforward to show that

Virtual processes (represented by $P/(E - E')$, where P = principal part) cannot be written in the form (24) and do not cancel out.

An example is the inelastic excitation of

$3d^9 4p^2 s^{+1} L \epsilon' l'$. In LS coupling, scattering from $3d^9 4s \epsilon f$ gives for $l' = 2$ or 4 (approximately)

$$N_{l'LS}(E) \approx C_{l'} \pi^2 (3d|r|\epsilon f)^2 (2S+1)(2L+1) \begin{Bmatrix} L & l' & 1 \\ 3 & 2 & 1 \end{Bmatrix} \times |R_1(\bar{\epsilon}f, 4s; \epsilon' l', 4p)|^2. \quad (29)$$

Here $C_2 = 2$, $C_4 = \frac{8}{3}$, $\epsilon = 4.12$ Ry, $\epsilon' = 4.22$ Ry, and $\bar{\epsilon}f$ stands for $\bar{R}_{\epsilon f}(r)$, where

$$\pi(3p|r|\epsilon f)\bar{R}_{\epsilon f}(r) = \int \frac{d\epsilon''(3d|r|\epsilon''f)}{\epsilon - \epsilon'' - i\delta} R_{\epsilon''f}(r). \quad (30)$$

Now $\text{Im}\bar{R}_{\epsilon f}(r) = R_{\epsilon f}(r)$. $\text{Re}\bar{R}_{\epsilon f}(r)$ can be found either directly by doing the principal value integration in (30) or by using the following trick. Let $\chi(r)/r$ be the real part of the right-hand side of (30). Then ($l=3$)

$$\frac{d^2\chi}{dr^2} + \left(\epsilon - U(r) - \frac{l(l+1)}{r^2} \right) \chi = r^2 R_{3d}(r). \quad (31)$$

If the right-hand side of (31) were zero, this would be the HS radial equation for $rR_{\epsilon l}(r)$. The solution of interest goes as r^{l+1} as $r \rightarrow 0$ and as $-\pi(3d|r|\epsilon f)/\sqrt{\pi k} \cos(kr + \theta_l)$ as $r \rightarrow \infty$ ($k = \sqrt{\epsilon}$). Numerical evaluation gives

$$R_1(\bar{\epsilon}f, 4s; \epsilon' d, 4p) = -0.175 \times 10^{-2} + 0.0795 i$$

and

$$R_1(\bar{\epsilon}f, 4s; \epsilon' g, 4p) = -0.0614 + 0.0207 i.$$

The total emission associated with $3d^9 4p$ is

$$\sum_{l'LS} N_{l'LS}(E) = 1.36 \times 10^{-2}$$

in units of $2\pi|\bar{E}_0|^2$ as before. The binding energies of the $\text{Cu}^+ 3d^9 4p$ states are in the interval 16 to 17 eV. The $3d^9 4s^2 {}^3F_J$ states occur at 16.4, 16.6, and 16.7 eV for $J=4, 3$, and 2 . The calculated $3d^9 4p$ intensity is larger than the calculated $3d^9 4s^2 {}^3F$ at resonance (0.64×10^{-2}). Hence a measurement of the 3F intensity could well include a large nonresonant background. In fact, recent experimental results confirm such an effect.⁹ Since $3p^6 3d^9 4p \epsilon' l'$ ($l' = 2$ or 4) presumably has no large matrix elements with discrete states of the form $3p^5 3d^{10} 4pnl$, there should be no interference effects (apart from those in $3d^9 4s$) in its excitation.

We have made similar estimates of the inelastic scattering from $3d^9 4s \epsilon l$ to $3d^9 4s^2 \epsilon' l'$. This is a much smaller effect. Only for $3d^9 4s^2 {}^1D$ is the (off-resonance) inelastic intensity comparable to the intensity due to sCK transitions. Here it is about 21% of the peak value (at resonance) and might be important experimentally. Also some interference could occur.

Turning to shake-up, let us determine the prob-

ability that emission from the $3d$ subshell results in the final-state ion configuration $3d^9 5s$ (instead of $3d^9 4s$). The $4s$ radial orbital $R_{4s}^I(r)$ in the ion differs from that of the ground state $R_{4s}^I(r)$. We find for HS orbitals

$$\int_0^\infty r^2 dr R_{4s}^{II}(r) R_{4s}^I(r) = 0.968$$

and

$$\int_0^\infty r^2 dr R_{5s}^{II}(r) R_{4s}^I(r) = -0.236.$$

Hence, if we treat the remaining orbitals as passive, we expect the main line ($3d^9 4s$) to have $(0.968)^2 = 93.7\%$ of the intensity and the $5s$ shake-up probability ($3d^9 5s$) to be $(-0.236)^2 = 5.6\%$.

Likewise, we find

$$\int_0^\infty r^2 dr R_{3d}^{II}(r) R_{3d}^I(r) = 0.9969$$

and

$$\int_0^\infty r^2 dr R_{4d}^{II}(r) R_{3d}^I(r) = -0.0512.$$

The $4d$ shake-up probability ($3d^9 4s 4d$) is $9 \times (-0.0512)^2 = 2.4\%$. The main line ($3d^9 4s$) is $[(0.9969)^2] = 94.6\%$ if we treat the $4s$ and other orbitals as passive. Overall, the $3d^9 4s$ main line has $93.7\% \times 94.6\% = 88.6\%$ of the intensity which is computed when shake-up is ignored. We do not expect this shake-up to affect the absorption (resonant or nonresonant) appreciably, but only to affect the binding-energy dependence of the photoemission. Near resonance the $3d^9 5s$ and $3d^9 4s 4d$ lines should show a Fano-type resonant behavior with $\bar{q} < q$, as discussed by Yafet.^{9,13} The binding energies of the $3d^9 5s$ states are in the range 21.1 to 21.4 eV.¹⁷ A broad photoemission peak is observed at about this energy⁹ and could be due to shake up as well as inelastic scattering into $3d^9 4s 4p$.

As a final topic, let us consider the effects of configuration interaction in all states (ground, discrete, and continuum). The most significant CI involves the $4p^2$ configuration.²³ In the ground state the matrix element between $3d^{10} 4s {}^2S$ and $3d^9 4p^2 {}^2S$ is (energies in Ry)

$$2(\frac{2}{3})^{1/2} R_1(4s, 3d; 4p, 4p) = -0.0488.$$

In HS, the energy denominator is

$$\epsilon_{4s} + \epsilon_{3d} - 2\epsilon_{4p} = -0.7615$$

and the coefficient of the $3d^9 4p^2$ component of Φ_r is 0.0641 (in first-order perturbation theory). This corresponds to a probability of 0.41%. For the discrete state $3p^5 3d^{10} 4p^2 {}^2P$, the matrix element with $3p^5 3d^{10} 4s^2 {}^2P$ is

$$-\frac{2}{\sqrt{3}}R_1(4p, 4p; 4s, 4s) = -0.1327$$

using the orbitals from the ground-state HS potential. The energy denominator is

$$2\epsilon_{4p} - 2\epsilon_{4s} = 0.5209$$

so that the coefficient of $3p^5 3d^{10} 4s^2$ in $3p^5 3d^{10} 4p^2$ is 0.2547. Owing to this mixing, $3p^5 3d^{10} 4p^2$ has a small oscillator strength equal to $(0.2547)^2 f_{3p \rightarrow 4s} = 4.0 \times 10^{-3}$, which is comparable to $f_{3p \rightarrow 4d}$. Also, there is a contribution from the $3d^9 4p^2$ component of Φ_g which involves $\langle 3p | r | 3d \rangle$, but it is an order of magnitude smaller. The energy of $3p^5 3d^{10} 4p^2$ must be roughly $0.52 \text{ Ry} \approx 7 \text{ eV}$ greater than $3p^5 3d^{10} 4s^2$ and could possibly contribute to the weak structure above the $3p \rightarrow 4s$ threshold.

In the final state, $3d^9 4s^2$ and $3d^8 4p^2$ mix with the same matrix element as above. It would be difficult, however, to observe any emission from $3d^8 4p^2$ due to this mixing, since 6.5% of the $3d^8 4s^2$ emission is rather small (1.4×10^{-3} at resonance). Likewise, the $3d^8 4p^2$ emission due to the admixture of $3d^9 4p^2$ in Φ_g is small ($\sim 8 \times 10^{-4}$). Yet another mixture, $3d^9 4s$ and $3d^8 4p^2$, would also give comparably small emission. Finally, the squared amplitude of $3d^9 4s \ ^1D$ mixed into $3d^8 4s^2$ (1D) is $\sim 10^{-4}$ and is of no consequence here.

IV. CONCLUSIONS

We have calculated the photoemission and photoabsorption of Cu in the region of the $3p \rightarrow 4s$ transition ($\sim 75 \text{ eV}$). We have used an independent particle model (HS radial orbitals) and a Fano-type formalism for the interference between $\Phi_g \rightarrow 3d^9 4s \epsilon l$ and $\Phi_g \rightarrow 3p^5 3d^{10} 4s n l'$ ($n l' = 4s, 5s, 4d, \dots$) followed by autoionization. The intensity of the

$3p \rightarrow 4s$ peaks relative to σ_{3d} agree fairly well (to within a factor of 2) with the absorption data of Bruhn, Sonntag, and Wolff.⁵ The relative oscillator strengths of $3p \rightarrow 4s, 5s, 4d$ are also consistent with the data. The calculated sCK width is ~ 2 too large, as noted previously by McGuire.¹⁵

The principal sCK decay of $3p^5 3d^{10} 4s^2$ is to $3d^9 4s^2 \ ^1G$ with lesser intensity in 3F and 1D . Auger decay to $3d^9 4s$ is weak enough that the calculated Fano asymmetry parameter is large ($q \sim 27$), indicating little interference. Inelastic scattering in the final state from $3d^9 4s \epsilon f$ to $3d^9 4p \epsilon' d, g$ is significant because this emission occurs at about the same binding energy as $3d^9 4s^2 \ ^3F$, providing a nonresonant background comparable to the sCK rate at resonance. At slightly higher binding energy, shake-up processes involving $3d^9 5s$ are predicted to have similar intensity.

It has been concluded that interference in the $\Phi_g \rightarrow 3p^5 3d^{10} 4s \epsilon d$ channel due to autoionization to $3p^6 3d^9 4s \epsilon' f$ causes the dip in the absorption observed by Bruhn *et al.* above the $3p \rightarrow 4s$ peaks. The calculated q value is small (~ 0.7) indicating strong interference and the one-electron cross section $\sigma_{3p \rightarrow \epsilon d}$ is relatively large (5% of σ_{3d}), resulting in an effect of the correct magnitude. It has been shown that $3p \rightarrow ns$ transitions, although relatively strong, do not cause appreciable interference. Transitions of the type $3p \rightarrow nd$ also have small q values, but most of the oscillator strength (at least for the HS potential) is in the continuum. Various other mechanisms have been considered and ruled out.

The authors wish to thank Dr. Y. Petroff for communicating experimental results prior to publication and Dr. Y. Yafet for helpful correspondence.

¹R. E. Dietz, E. G. McRae, Y. Yafet, and C. W. Caldwell, *Phys. Rev. Lett.* **33**, 1372 (1974).

²J. P. Connerade, M. W. D. Mansfield, and M. A. P. Martin, *Proc. R. Soc. London Ser. A* **350**, 405 (1976); R. Bruhn, B. Sonntag, and H. W. Wolff, *Phys. Lett.* **69A**, 9 (1978).

³L. C. Davis and L. A. Feldkamp, *Phys. Rev. A* **17**, 2012 (1978).

⁴F. Combet Farnoux and M. Ben Amar, *Phys. Rev. A* **21**, 1975 (1980).

⁵R. Bruhn, B. Sonntag, and H. W. Wolff, *J. Phys. B* **12**, 203 (1979).

⁶U. Fano, *Phys. Rev.* **124**, 1866 (1961).

⁷E. J. McGuire, *Phys. Rev. A* **5**, 1052 (1972); *J. Phys. Chem. Solids* **33**, 577 (1972).

⁸Y. Yafet, *Phys. Rev. B* **23**, 3558 (1981).

⁹D. Chandesaris, C. Guillof, G. Chauvin, J. Lecante, and Y. Petroff (unpublished).

¹⁰F. Herman and S. Skillman, *Atomic Structure Calculations* (Prentice-Hall, Englewood Cliffs, 1963).

¹¹L. C. Davis and L. A. Feldkamp, *Phys. Rev. B* **15**, 2961 (1977).

¹²L. C. Davis and L. A. Feldkamp, *Phys. Rev. B* **23**, 6239 (1981).

¹³Y. Yafet, *Phys. Rev. B* **21**, 5023 (1980).

¹⁴Since the HS wave functions are only an approximation to the (correct) HF wave functions, we have not attempted to evaluate matrix elements to high accuracy. Our results are typically accurate to 1%.

¹⁵E. J. McGuire, *Phys. Rev. A* **16**, 2365 (1977).

¹⁶A. F. Starace, *Appl. Opt.* **19**, 4051 (1980).

¹⁷C. E. Moore, *Atomic Energy Levels*, NSRDS-NBS 35 (U. S. GPO, Washington, D. C., 1971), Vol. II. Also see C. B. Ross, Los Alamos Scientific Laboratory Report No. LA-4498 (unpublished).

¹⁸D. A. Shirley, R. L. Martin, S. P. Kowalczyk, F. R.

McFeely, and L. Ley, Phys. Rev. B 15, 555 (1977).

¹⁹S. T. Manson and J. W. Cooper, Phys. Rev. 165, 126 (1968).

²⁰To justify this treatment, we refer to Ref. 12. The first model considered in that paper is formally equivalent to the present problem (empty d bands become the continuum). If we neglect the small quantity $F_I - i\Gamma_i$ in $h(E, -i\pi)$ [Eq. (3.36)], then Eq. (3.45) results in the form given by Eq. (22) of the present work.

²¹D. J. Kennedy and S. T. Manson, Phys. Rev. A 5, 227

(1972).

²²G. Wendin, J. Phys. B 3, 455 (1970); 3, 466 (1970); 4, 1080 (1971); 5, 110 (1972); 6, 42 (1973); *Vacuum Ultraviolet Radiation Physics*, edited by E. E. Koch, R. Haensel, and C. Kunz (Vieweg-Pergamon, Berlin, 1974), p. 225; Daresbury Nuclear Laboratory Report No. DL/SCI/R11 (unpublished); Struct. Bonding (Berlin) (in press).

²³C. Froese Fischer and J. S. Carley, J. Phys. B 9, 29 (1976).